Downloaded from orbit.dtu.dk on: Jun 09, 2023

DTU Library

The Inclusion of HVDC Control Modes in a Three-Phase Newton-Raphson Power Flow Algorithm

Coffele, Federico; Garcia-Valle, Rodrigo; Acha, Enrique

Published in:
IEEE PowerTech

Link to article, DOI:
10.1109/PCT.2007.4538354

Publication date:
2007

Document Version
Publisher's PDF, also known as Version of record

Link back to DTU Orbit

Citation (APA):
Coffele, F., Garcia-Valle, R., & Acha, E. (2007). The Inclusion of HVDC Control Modes in a Three-Phase Newton-Raphson Power Flow Algorithm. In *IEEE PowerTech* PES - IEEE.
https://doi.org/10.1109/PCT.2007.4538354

General rights
Copyright and moral rights for the publications made accessible in the public portal are retained by the authors and/or other copyright owners and it is a condition of accessing publications that users recognise and abide by the legal requirements associated with these rights.

- Users may download and print one copy of any publication from the public portal for the purpose of private study or research.
- You may not further distribute the material or use it for any profit-making activity or commercial gain
- You may freely distribute the URL identifying the publication in the public portal

If you believe that this document breaches copyright please contact us providing details, and we will remove access to the work immediately and investigate your claim.

THE INCLUSION OF HVDC CONTROL MODES IN A THREE-PHASE NEWTON-RAPHSON POWER FLOW ALGORITHM

Federico Coffele, Rodrigo J. Garcia-Valle, *Member, IEEE,* and Enrique Acha, *Senior Member, IEEE*

***Abstract*— A three-phase Newton-Raphson power flow algorithm with conventional HVDC power plant modelling is presented in this paper. Emphasis is placed on the representation of converter control modes. The solution approach takes advantage of the strong numerical convergence afforded by the Newton-Raphson method in polar coordinates to yield reliable numerical solutions for combined HVAC-HVDC systems, where power plant and operational imbalances are explicitly taken into account. Although well-developed algorithms exist for solving fundamental frequency, three-phase power flows or combined power flows/harmonic currents, no HVDC converter control mode representation appears to have been addressed in the numerically reliable three-phase Newton-Raphson method. Two test cases are solved, one corresponding to a small system to enable reproduction of results by interested readers and the other is a large system containing several HVDC links and operational control modes.**

***Index Terms*— Three-phase power flows, Newton-Raphson method, HVDC transmission control.**

I. INTRODUCTION

Over many years, interest in HVDC technology for bulk power transmission, and other more specialised applications, has remained strong. Further to the traditional HVDC technology, termed line commutated current (LCC), based on the use of conventional thyristors; two other lines of development in HVDC technology have appeared, capacitor commutated converters (CCC), which is an upgrading of the traditional technology, and voltage source converters (VSC) with insulated gate bipolar transistor (IGBT) and pulse width modulation (PWM) control. In each of these applications, manufactures have taken maximum benefits from the accelerated pace of power electronics technology. It is believed that in a few years time, HVDC-VSC-based systems, will take over a large portion of the traditional HVDC market. However at present, bulk power DC transmission remains the realm of thyristor-based HVDC technology [1].

The need for bulk power exchanges between grids separated by the sea increases the worth of classical HVDC, where at present, it has no direct competitor. A case in point is the 600 MW HVDC link to be licensed in 2007 joining the British and the Dutch power grids; with a doubling of the link capacity projected by 2010 [2]. Moreover, interest in HVDC transmission in the UK goes beyond the niche markets of HVDC; owing to the need to preserve the environment and countryside, HVDC is becoming attractive in situations where AC high voltage transmission was considered the de facto option, such as the 400 kV transmission line to be built between Beauly and Denny, across the Scottish highlands. The HVDC option, with its smaller footprint's towers, is much preferred by environmentalist presume groups.

In large conurbation centres, utility planners are actively considering the viability of reconverting existing AC transmission corridors into HVDC lines to take advantage of the higher power density achieved with the latter. To make informed decisions, however, power systems applications tools with suitable HVDC representation are not only desirable but essential. Power flows is the most basic tool with which to study the system level performance of combined HVDC-HVAC systems and although a fair amount of work has been published in the representation of HVDC links in positive sequence power flows, relatively little work has been published in HVDC link modelling in three-phase power flows, where the network voltage imbalances and their impact on HVDC converter plant play a key role. In fact, the main line of development that has been published in this area belongs to the Fast Decoupled power flow method, dealing with either fundamental frequency power flows solutions [3], [4], or combined fundamental frequency power flows/harmonic currents solutions carried out in a sequential manner [5]. However, as stated in [6], the approach may take a substantial number of iterations to converge; the reasons being the sequential nature of the approach and the linear convergence characteristics, as opposed to quadratic, of the Fast Decoupled method. Hence, steps have been taken to solve the combined fundamental frequency power flows/harmonic currents solutions in a unified manner using a full Newton-Raphson method in rectangular coordinates to yield quadratic solutions [6]. However, the key issue of HVDC converter control mode representation is not addressed and the approach is unduly complex if the interest is not in power converter harmonics but only in fundamental frequency, three-phase power flow solutions. This paper deals with HVDC converter control mode representation in three-phase power flows, and a Newton-Raphson polar formulation has been selected for development as opposed to the rectangular version.

Mr. Coffele is with the Department of Electrical Engineering, University of Padova, Italy.

Mr. Garcia-Valle and Dr. Acha are with Department of Electronics and Electrical Engineering, University of Glasgow, G12 8LT U.K. (e-mail: rgarcia@elec.gla.ac.uk)

Authorized licensed use limited to: Danmarks Tekniske Informationscenter. Downloaded on February 25, 2009 at 10:38 from IEEE Xplore. Restrictions apply.

II. HVDC MODELLING

The monopolar HVDC transmission system scheme, shown in Fig. 1, is used in this paper to explain the model developed and its inclusion in a three-phase power flow using the full Newton-Raphson method. However, the approach is quite general and it can easily be expanded to include some of the most common HVDC configurations, such as bipolar HVDC systems.

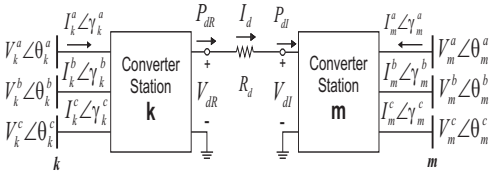

Fig. 1. Monopolar HVDC system.

In the monopolar HVDC link, two converter stations are joined together by a line conductor, and the earth (sea) is used as the return path, requiring two electrodes capable of carrying the full current. In addition to the six pulse bridge, each converter station comprises a three-phase tap-changing transformer (LTC).

A. Three-Phase Power Equations

To derive the power flow Newton-Rapshon model, the three-phase power consumed by the converters is written as a function of AC voltages and DC variables.

$$P_k^\rho = f\left(V_k^{a,b,c}, \theta_k^{a,b,c}, X\right) \tag{1}$$

$$P_m^\rho = f\left(V_m^{a,b,c}, \theta_m^{a,b,c}, X\right) \tag{2}$$

where P_k and P_m are active powers at buses k and m, respectively; V_k and θ_k and V_m and θ_m are the voltage magnitudes and phase angles, respectively, at the sending and receiving buses k and m; ρ denotes the a, b, and c phases of the system. X represents, in generic form at this stage, the DC variables.

The reactive powers are

$$Q_k^\rho = \sqrt{(S_k^\rho)^2 - (P_k^\rho)^2} = \sqrt{\frac{\left(k_1 A_k V_k^\rho I_d\right)^2}{3} - (P_k^\rho)^2} \tag{3}$$

$$Q_m^\rho = \sqrt{(S_m^\rho)^2 - (P_m^\rho)^2} = \sqrt{\frac{\left(k_1 A_m V_m^\rho I_d\right)^2}{3} - (P_m^\rho)^2} \tag{4}$$

where S_k and Q_k and S_m and Q_m are the apparent and reactive powers at buses k and m respectively; k_1 is a constant associated with the commutation overlap, A_k and A_m are the tap-changers positions at buses k and m, respectively; and I_d is the current in the dc-link. The full derivation is given in Appendix I.

III. LINEARISED POWER EQUATIONS

A three-phase power network with n-buses is described by $6 \times (n-1)$ non linear equations. The inclusion of one HVDC link in the network model augments the number of equations by six. The solution of the combined system of non-linear equations is carried out by iteration using the full Newton Raphson method.

The power through the DC link can be controlled by varying the DC-voltages, as indicated by the following two basic relations:

$$P_{dR} = V_{dR} I_d \tag{5}$$

$$P_{dI} = V_{dI} I_d \tag{6}$$

where P_{dR} and P_{dI} are the DC powers at the inverter and rectifier ends, respectively; and V_{dR} and V_{dI} are the DC voltages, at the rectifier and inverter, respectively.

The DC-voltages can be controlled either with the transformers tap ratios or with the converters control angles. At the rectifier, the control angle is the firing angle α; and at the inverter, the control angle is the extinction angle, γ. An increase in the control angle gives a decrease in DC-voltage, an increase in reactive power consumption (since the current will lag the voltage) and an increase in harmonics generation. The latter is clearly undesirable and there is thus some benefit in keeping the control angles at low values [7].

There are several modes of operation in converter control. The first one, when the firing angle α, the extinction angle γ, V_{dI} and P_{dI} are specified, is called control mode A. The converter transformer taps are varied in order to meet these specifications. In control mode B, the extinction angle γ, is kept at its lower limit at the inverter and the transformer taps and the power P_{dI} are specified. The power is controlled by varying the firing angle α at the rectifier. The firing angle rather than the tap transformer is preferred for control, since the tap changer control is too slow compared to the firing angle. In control mode C, α is fixed to its minimum value and γ is regulated to maintain constant power.

If the current I_d is kept constant instead of the power P_{dI}, three other control modes are defined. In this paper only the mode A, B and C with constant power are addressed.

The Jacobian used in conventional power flows is suitably extended to take account of the new elements contributed by the HVDC link. The set of linearised power flow equations for the complete system is,

$$\begin{bmatrix} \Delta P \\ \Delta Q \\ -- \\ \Delta P_{dR} \\ \Delta P_{dI} \end{bmatrix} = \begin{bmatrix} \boldsymbol{J_{11}} & | & \boldsymbol{J_{12}} \\ -- & + & -- \\ \boldsymbol{J_{21}} & | & \boldsymbol{J_{22}} \end{bmatrix} \begin{bmatrix} \Delta\theta \\ \frac{\Delta V}{V} \\ -- \\ \Delta X_1 \\ \Delta X_2 \end{bmatrix} \tag{7}$$

where

$\Delta P = [\Delta P_1^\rho, \cdots, \Delta P_n^\rho]^t$
$\Delta Q = [\Delta Q_1^\rho, \cdots, \Delta Q_n^\rho]^t$
$\Delta\theta = [\Delta\theta_1^\rho, \cdots, \Delta\theta_n^\rho]^t$
$\frac{\Delta V}{V} = \left[\frac{\Delta V_1^\rho}{V_1^\rho}, \cdots, \frac{\Delta V_n^\rho}{V_n^\rho}\right]^t$

ΔP and ΔQ are the normal power mismatch equations,

Authorized licensed use limited to: Danmarks Tekniske Informationscenter. Downloaded on February 25, 2009 at 10:38 from IEEE Xplore. Restrictions apply.

and $\Delta\theta$ and $\frac{\Delta V}{V}$ are voltage increments of phase angle and magnitude, respectively.

There are two additional state variables X_1 and X_2, (i.e. $X_{1,2}$), and two power mismatch equations introduced by the HVDC link,

$$\Delta P_{dR} = P_{dR}^{sch} - P_{dR}^{cal} \quad (8)$$

$$\Delta P_{dI} = P_{dI}^{sch} - P_{dI}^{cal} \quad (9)$$

P^{sch} and P^{cal} are the scheduled and calculated powers for the HVDC link.

The power mismatches for buses k and m, where the HVDC link is connected to become:

$$\Delta P_k = P_{Gk} - P_{Lk} - P_{Nk}(\theta, V) - P_{dR}(V_k, V_m, X_{1,2}) \quad (10)$$

$$\Delta P_m = P_{Gm} - P_{Lm} - P_{Nm}(\theta, V) - P_{dI}(V_k, V_m, X_{1,2}) \quad (11)$$

$$\Delta Q_k = Q_{Gk} - Q_{Lk} - Q_{Nk}(\theta, V) - Q_{dR}(V_k, V_m, X_{1,2}) \quad (12)$$

$$\Delta Q_m = Q_{Gm} - Q_{Lm} - Q_{Nm}(\theta, V) - Q_{dI}(V_k, V_m, X_{1,2}) \quad (13)$$

where P_{Gk}, Q_{Gk} and P_{Gm} and Q_{Gm} represent the active and reactive powers injected by the generator at buses k and m, respectively; P_{Lk}, Q_{Lk} and P_{Lm} and Q_{Lm} represent the active and reactive powers drawn by the load at buses k and m, respectively;

The J_{11} matrix corresponding to the AC network at buses k and m

$$\begin{bmatrix} \frac{\partial P_k^\rho}{\partial \theta_k^\rho} & \frac{\partial P_k^\rho}{\partial V_k^\rho} V_k^\rho & \frac{\partial P_k^\rho}{\partial \theta_m^\rho} & \frac{\partial P_k^\rho}{\partial V_m^\rho} V_m^\rho \\ \frac{\partial Q_k^\rho}{\partial \theta_k^\rho} & \frac{\partial Q_k^\rho}{\partial V_k^\rho} V_k^\rho & \frac{\partial Q_k^\rho}{\partial \theta_m^\rho} & \frac{\partial Q_k^\rho}{\partial V_m^\rho} V_m^\rho \\ \frac{\partial P_m^\rho}{\partial \theta_k^\rho} & \frac{\partial P_m^\rho}{\partial V_k^\rho} V_k^\rho & \frac{\partial P_m^\rho}{\partial \theta_m^\rho} & \frac{\partial P_m^\rho}{\partial V_m^\rho} V_m^\rho \\ \frac{\partial Q_m^\rho}{\partial \theta_k^\rho} & \frac{\partial Q_m^\rho}{\partial V_k^\rho} V_k^\rho & \frac{\partial Q_m^\rho}{\partial \theta_m^\rho} & \frac{\partial Q_m^\rho}{\partial V_m^\rho} V_m^\rho \end{bmatrix} \quad (14)$$

is augmented with the partial derivatives of the active and reactive powers contributions by the HVDC link.

Matrix J_{12} includes the partial derivatives of the three-phase powers $P_{k,m}^\rho$ and $Q_{m,n}^\rho$ with respect to the HVDC link state variables and J_{21} represents the partial derivatives of P_{dR} and P_{dI} with respect to the three-phase voltage angles and magnitudes $\theta_{k,m}^\rho$ and $V_{k,m}^\rho$. Moreover, J_{22} represents the self partial derivatives of the HVDC link.

A. Control mode A

In control mode A, the variables α, γ, V_{dI} and P_{dI} are specified, making it possible to calculate the current I_d, the voltage V_{dI} and the power P_{dR}:

$$I_d = \frac{P_{dI}}{V_{dI}} \quad (15)$$

$$V_{dR} = V_{dI} + R_{DC} I_d \quad (16)$$

$$P_{dR} = V_{dR} I_d \quad (17)$$

The new state variables for this control mode are the tap changers, A_k and A_m, with the Jacobian elements J_{12}, J_{21} and J_{22} having the following structure:

$$J_{12} = \begin{bmatrix} \frac{\partial P_k^\rho}{\partial A_k} & \frac{\partial P_k^\rho}{\partial A_m} \\ \frac{\partial Q_k^\rho}{\partial A_k} & \frac{\partial Q_k^\rho}{\partial A_m} \\ \frac{\partial P_m^\rho}{\partial A_k} & \frac{\partial P_m^\rho}{\partial A_m} \\ \frac{\partial Q_m^\rho}{\partial A_k} & \frac{\partial Q_m^\rho}{\partial A_m} \end{bmatrix} \quad (18)$$

$$J_{21} = \begin{bmatrix} \frac{\partial P_{dR}}{\partial \theta_k^\rho} & \frac{\partial P_{dR}}{\partial V_k^\rho} V_k^\rho & \frac{\partial P_{dR}}{\partial \theta_m^\rho} & \frac{\partial P_{dR}}{\partial \theta_m^\rho} V_m^\rho \\ \frac{\partial P_{dI}}{\partial \theta_k^\rho} & \frac{\partial P_{dI}}{\partial V_k^\rho} V_k^\rho & \frac{\partial P_{dI}}{\partial \theta_m^\rho} & \frac{\partial P_{dI}}{\partial \theta_m^\rho} V_m^\rho \end{bmatrix} \quad (19)$$

$$J_{22} = \begin{bmatrix} \frac{\partial P_{dR}}{\partial A_k} & \frac{\partial P_{dR}}{\partial A_m} \\ \frac{\partial P_{dI}}{\partial A_k} & \frac{\partial P_{dI}}{\partial A_m} \end{bmatrix} \quad (20)$$

It should be noted that a single tap-changer is used to regulate voltage magnitude at all three phases.

B. Control mode B

In control mode B, the variables a_k, a_m, γ and P_{dI} are specified and the new state variables are the current I_d and the firing angle α. For this control mode, J_{21} has the same structure as in control mode A. The other two terms of the Jacobian are:

$$J_{12} = \begin{bmatrix} \frac{\partial P_k^\rho}{\partial \alpha} & \frac{\partial P_k^\rho}{\partial I_d} \\ \frac{\partial Q_k^\rho}{\partial \alpha} & \frac{\partial Q_k^\rho}{\partial I_d} \\ \frac{\partial P_m^\rho}{\partial \alpha} & \frac{\partial P_m^\rho}{\partial I_d} \\ \frac{\partial Q_m^\rho}{\partial \alpha} & \frac{\partial Q_m^\rho}{\partial I_d} \end{bmatrix} \quad (21)$$

$$J_{22} = \begin{bmatrix} \frac{\partial P_{dR}}{\partial \alpha} & \frac{\partial P_{dR}}{\partial I_d} \\ \frac{\partial P_{dI}}{\partial \alpha} & \frac{\partial P_{dI}}{\partial I_d} \end{bmatrix} \quad (22)$$

C. Control mode C

In control mode C, the variables a_k, a_m, α and P_{dI} are specified and the new state variables are the current I_d and the extinction angle γ. Matrix J_{21} has the same structure as in the previous control modes, whereas matrices J_{12} and J_{22} take the following structure,

$$J_{12} = \begin{bmatrix} \frac{\partial P_k^\rho}{\partial I_d} & \frac{\partial P_k^\rho}{\partial \gamma} \\ \frac{\partial Q_k^\rho}{\partial I_d} & \frac{\partial Q_k^\rho}{\partial \gamma} \\ \frac{\partial P_m^\rho}{\partial I_d} & \frac{\partial P_m^\rho}{\partial \gamma} \\ \frac{\partial Q_m^\rho}{\partial I_d} & \frac{\partial Q_m^\rho}{\partial \gamma} \end{bmatrix} \quad (23)$$

$$J_{22} = \begin{bmatrix} \frac{\partial P_{dR}}{\partial I_d} & \frac{\partial P_{dR}}{\partial \gamma} \\ \frac{\partial P_{dI}}{\partial I_d} & \frac{\partial P_{dI}}{\partial \gamma} \end{bmatrix} \quad (24)$$

It is important to remark that this is a three-phase formulation, and that all elements in the above equations are vectors of order 3×1, except for J_{11} which are vectors of order 3×3 and J_{22} which are single terms.

Authorized licensed use limited to: Danmarks Tekniske Informationscenter. Downloaded on February 25, 2009 at 10:38 from IEEE Xplore. Restrictions apply.

IV. Numerical examples

A. Test Case 1

To show the applicability of the proposed approach, the five-bus network depicted in Fig. 2 is used. All necessary data to carry out a balanced three-phase AC power flow is taken from [8].

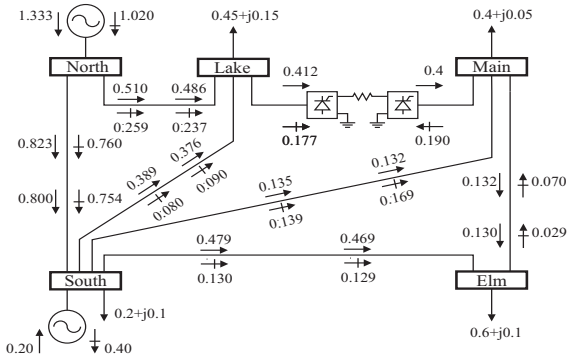

Fig. 2. Five-bus test network for three-phase balanced conditions.

The five-bus network is modified to include one HVDC link connected between Lake and Main buses. In this contrived example, the AC network and HVDC converters are assumed to work under three-phase balanced conditions. The HVDC link is made to operate in control mode A.

The data used for the HVDC link is given at Table I and the three-phase nodal voltage magnitudes and phase angles are given in Table II. Notice that voltage values are given in per unit and angles are given in degrees.

TABLE I
DATA FOR THE HVDC LINK.

Transformer reactances	0.051 pu
D.C. link resistance	0.10 pu
Firing angle for the rectifier	15 deg
Extinction angle for the inverter	18 deg
Transmitted power	0.4 pu per phase

TABLE II
BUS VOLTAGES AND GENERATION RESULTS.

Bus name	Phase A		Phase B		Phase C	
	Voltage	Angle	Voltage	Angle	Voltage	Angle
North	1.060	0	1.060	-120	1.060	120
South	1.000	-1.8126	1.000	-121.8126	1.000	118.1874
Lake	0.9610	-5.5998	0.9610	-125.5998	0.9610	114.4002
Main	0.9634	-2.6911	0.9634	-122.6911	0.9634	117.3089
Elm	0.9648	-4.8845	0.9648	-124.8845	0.9648	115.1155

Table III shows the generated powers in the North and South buses, and the powers in both the rectifier and the inverter, which are connected to Lake and Main, respectively. All other active and reactive power flows are shown in Fig. 2, for phase A only.

TABLE III
POWERS FROM GENERATOR BUSES AND HVDC CONVERTERS.

	HVDC converter				Generator buses			
	Main		Lake		North		South	
	P	Q	P	Q	P	Q	P	Q
Phase A	0.40	0.1902	0.412	0.1772	1.333	1.02	0.20	-0.4053
Phase B	0.40	0.1902	0.412	0.1772	1.333	1.02	0.20	-0.4053
Phase C	0.40	0.1902	0.412	0.1772	1.333	1.02	0.20	-0.4053

B. Test Case 2

To show the wider applicability of this technique, the New England test system [9], which consists of 68 nodes, 16 generators and 86 transmission lines, is used.

The system has been modified to include three HVDC links, each operating with a different operational control mode, as described in Table IV.

TABLE IV
HVDC LINK CONTROL MODES.

	from	to	Control mode
Link 1	bus 41	bus 42	C
Link 2	bus 1	bus 27	A
Link 3	bus 23	bus 24	B

Imbalances are introduced into the network by changing the active and reactive power loads at the buses where the HVDC stations connect, by $\pm 10\%$ with respect to the balanced case. Phase A is subtracted 10%, Phase B is added 10% and Phase C is kept unchanged.

Tables V, VI and VII show the unbalanced three-phase voltage profiles and the active and reactive powers for each HVDC converter. The solution was achieved in 6 iterations to a power mismatch tolerance of $1e^{-12}$.

TABLE V
PARAMETERS OF LINK 1.

	Sending Node			Receiving Node		
	A	B	C	A	B	C
$\|V\|$	0.9941	0.9942	0.9941	0.9973	0.9976	0.9966
θ	47.1452	-71.7897	167.0982	18.8528	-102.6938	136.3634
P	0.4428	0.4401	0.4430	0.3940	0.4012	0.4048
Q	0.3255	0.3292	0.3253	0.3857	0.3784	0.3737

TABLE VI
PARAMETERS OF LINK 2.

	Sending Node			Receiving Node		
	A	B	C	A	B	C
$\|V\|$	0.9992	1.0015	1.0024	0.9845	1.0014	0.9899
θ	-5.6705	-125.4563	114.6696	-6.6707	-124.6575	116.1454
P	0.3561	0.3566	0.3567	0.3342	0.3361	0.3297
Q	0.2196	0.2205	0.2211	0.2234	0.2329	0.2338

Authorized licensed use limited to: Danmarks Tekniske Informationscenter. Downloaded on February 25, 2009 at 10:38 from IEEE Xplore. Restrictions apply.

TABLE VII
PARAMETERS OF LINK 3.

	Sending Node			Receiving Node		
	A	B	C	A	B	C
$\|V\|$	1.0113	1.0142	1.0142	0.9696	0.9822	0.9749
θ	9.0899	-109.0112	131.4502	-6.1403	-124.4343	116.5493
P	0.6372	0.6295	0.6270	0.5354	0.5374	0.5272
Q	0.6252	0.6366	0.6391	0.5692	0.5812	0.5826

The three HVDC links are set to operate with different control schemes and the state variables are A_k and A_m (control mode A) for link 1; α and I_d (control mode B) for link 2; and γ and I_d (control mode C) for link 3.

Figures 3, 4 and 5 show the behaviour towards the convergence for each state variable during the power flow solution.

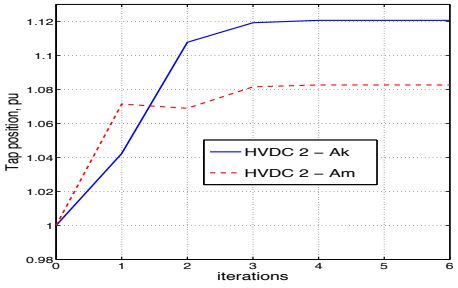

Fig. 3. Tap position of link 2, Control Mode A.

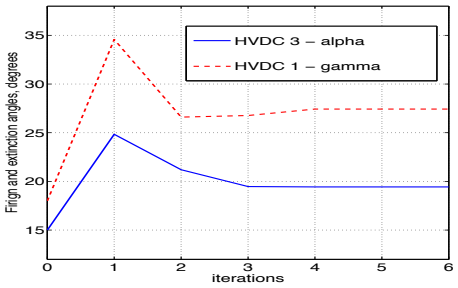

Fig. 4. Firing and extinction angles of links 3 and 1, Control Mode B and C, respectively.

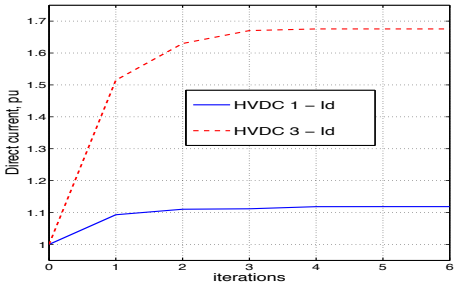

Fig. 5. Direct current of links 1 and 3, Control Mode B and C, respectively.

It should be noticed that the state variables A_k, A_m and I_d have initial values of 1 per unit, and upon convergence, settle to final values. For the remaining state variables, α and γ, are given values of 15° and 18° degrees, respectively, which are typical specified control angles [10], [3].

V. CONCLUSIONS

This paper presents a three-phase power flow method to include conventional HVDC link models where several control modes are applied. The approach takes advantage of the strong convergence characteristics of the full Newton-Raphson technique to ensure reliable iterative solutions. Two non-linear equations per HVDC link, in linearised form, are combined with the linearised equations of the rest of the power system for unified, iterative solutions that yield quadratic convergence. Two test cases have been presented, one correspond to a simple network with one HVDC link and operating under balanced conditions. This should enable interested readers to reproduce results with ease. The other is a large network including unbalanced loading and three HVDC links; each operating with its own control mode. The implementation of the proposed technique can be expanded to include other HVDC configurations, such as bipolar and multi-terminal HVDC systems.

ACKNOWLEDGEMENTS

The authors gratefully acknowledge the financial assistance given to Mr. Coffele by the University of Padova, Italy to carry out his specialisation degree thesis and to Mr. Garcia-Valle by the Consejo Nacional de Ciencia y Tecnologia, Mexico to carry out Ph.D. studies at the University of Glasgow, UK.

REFERENCES

[1] L. Carlsson, "Classical HVDC: Still continuing to evolve," *Modern Power Systems, MPS Review: Transmission & Distribution*, pp. 19–21, June 2002.
[2] National Grid Company plc, "Interim Great Britain seven year statement." [Online]. Available: http://www.nationalgrid.com/uk
[3] J. Arrillaga and C. P. Arnold, *Computer Analysis of Power Systems*. John Wiley & Sons, Inc., 1990.
[4] B. J. Harker and J. Arrillaga, "3-phase ac-dc load flow," *IEE Proceedings*, vol. 126, pp. 1275–1281, December 1979.
[5] J. Arrillaga and C. D. Callaghan, "Three phase ac-dc load and harmonics flows," *IEEE Transactions on Power Delivery*, vol. 6, pp. 238–241, January 1991.
[6] J. Arrillaga, N. Watson, and G. Bathrust, "A multifrequency power flow of general applicability," *IEEE Transactions on Power Delivery*, vol. 19, pp. 342–349, January 2004.
[7] J. Arrillaga, *High Voltage Direct Current Transmission*. IEE Power and Energy Series, 1998.
[8] E. Acha, C. R. Fuerte-Esquivel, H. Ambriz-Perez, and C. Angeles-Camacho, *FACTS Modelling and Simulation in Power Networks*. John Wiley & Sons, Inc., 2004.
[9] J. H. Chow, *Time-Scale Modeling of Dynamic Networks with Applications to Power Systems*. Springer-Verlag, 1982.
[10] E. T. Smed, "A new approach to ac/dc power flow," MSc. Thesis, Auburn University, December 1989.

Authorized licensed use limited to: Danmarks Tekniske Informationscenter. Downloaded on February 25, 2009 at 10:38 from IEEE Xplore. Restrictions apply.

APPENDIX I
HVDC POWER EQUATIONS

A standard six-pulse converter brindge is used to derive the mathematical model for the three-phase HVDC station. The three-phase supply voltages to the converter transformer v^a, v^b and v^c are taken to be unbalanced but sinusoidal, as shown in Fig. 6. The commutation is assumed to be delayed by an angle α with equidistant firing angle control [7], i.e. firing instants occur at successive intervals of 60° following the first voltage crossing.

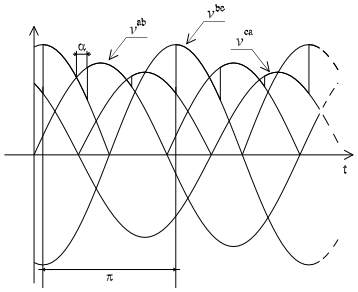

Fig. 6. Unbalanced converter voltage waveform.

From Fig. 6, the rectified voltage V_{dR} is obtained by integration,

$$V_{dR} = \frac{1}{\pi}\int_{\alpha}^{\alpha+\frac{\pi}{3}} \left[-v^{ca}(\theta)\right] d\theta + \frac{1}{\pi}\int_{\alpha+\frac{\pi}{3}}^{\alpha+\frac{2\pi}{3}} \left[v^{bc}(\theta)\right] d\theta + \frac{1}{\pi}\int_{\alpha+\frac{2\pi}{3}}^{\alpha+\pi} \left[-v^{ab}(\theta)\right] d\theta \tag{25}$$

The voltage V_{dR} is made up of three terms,

$$V_{dR} = V_{dR}^a + V_{dR}^b + V_{dR}^c \tag{26}$$

where

$$V_{dR}^a = \frac{A\sqrt{2}V^{ab}}{\pi}\left[\cos\left(\alpha+\frac{\pi}{3}\right) - \cos\left(\alpha+\frac{2\pi}{3}\right)\right] \tag{27}$$

$$V_{dR}^b = \frac{A\sqrt{2}V^{bc}}{\pi}\left[\cos\left(\alpha+\theta^{bc}-\pi\right) - \cos\left(\alpha+\theta^{bc}-\frac{2\pi}{3}\right)\right] \tag{28}$$

$$V_{dR}^c = \frac{A\sqrt{2}V^{ca}}{\pi}\left[\cos\left(\alpha+\theta^{ca}-\frac{\pi}{3}\right) - \cos\left(\alpha+\theta^{ca}\right)\right] \tag{29}$$

giving

$$V_{dR}^{\rho}\frac{A_k\sqrt{2}V_k^{\rho}}{\pi}\cos\left(\alpha+A^{\rho}\right) \tag{30}$$

where $A^a = \theta^{ab} = 0$, $A^b = \theta^{bc} - \frac{4\pi}{3}$ and $A^c = \theta^{ca} - \frac{2\pi}{3}$. A similar expression is developed for the inverter,

$$V_{dI}^{\rho} = \frac{A_m\sqrt{2}V_m^{\rho}}{\pi}\cos\left(\gamma+B^{\rho}\right) \tag{31}$$

where $B^a = \varphi^{ab} = 0$, $B^b = \varphi^{bc} - \frac{4\pi}{3}$ and $B^c = \varphi^{ca} - \frac{2\pi}{3}$. Taking into account the voltage drop ΔV, the DC voltages of the rectifier and the inverter are:

$$V_{dR}^{\rho} = \frac{A_k\sqrt{2}V_k^{\rho}}{\pi}\cos\left(\alpha+A^{\rho}\right) - \Delta V \tag{32}$$

$$V_{dI}^{\rho} = \frac{A_m\sqrt{2}V_m^{\rho}}{\pi}\cos\left(\gamma+B^{\rho}\right) - \Delta V \tag{33}$$

where ΔV is defined as,

$$\Delta V = \frac{X_c I_d}{\pi} \tag{34}$$

The powers of the inverter and the rectifier are given by the following expressions,

$$P_{dR} = V_{dR}I_d = \sum_{\rho=a,b,c} V_{dR}^{\rho} I_d \tag{35}$$

$$P_{dI} = V_{dI}I_d = \sum_{\rho=a,b,c} V_{dI}^{\rho} I_d \tag{36}$$

The relations between the currents on the primary side of the three-phase transformers and the direct current I_d, are given by,

$$\begin{aligned} I_k^{\rho} &= A_k k\frac{\sqrt{6}}{\pi}I_d = A_k k I_d \\ I_m^{\rho} &= A_m k\frac{\sqrt{6}}{\pi}I_d = A_m k I_d \end{aligned} \tag{37}$$

where k is a constant associated with commutation overlap. For power flow analysis, it can be taken to be $k = 0.995$ [3].

The apparent powers are given by,

$$S_k^{\rho} = \frac{V_k^{\rho}I_k^{\rho}}{\sqrt{3}} = \frac{k_1 A_k V_k^{\rho} I_d}{\sqrt{3}} \tag{38}$$

$$S_m^{\rho} = \frac{V_m^{\rho}I_m^{\rho}}{\sqrt{3}} = \frac{k_1 A_m V_m^{\rho} I_d}{\sqrt{3}} \tag{39}$$

where $k_1 = \frac{\sqrt{6}}{\pi}k$

Federico Coffele was born in Italy. He was an Erasmus-Socrates student at the University of Glasgow, UK, in 2006. He graduated from the electrical engineering department at the University of Padova, Italy, in 2007.

Rodrigo Garcia-Valle was born in Mexico. He received the electrical engineering degree from ESIME, IPN, Mexico city, Mexico, in 2001 and the MSc degree from CINVESTAV, Guadalajara, Mexico, in 2003. Currently he is pursuing the PhD degree in electrical power systems at the University of Glasgow, UK.

Enrique Acha (SM'02) was born in Mexico. He graduated from Universidad Michoacana de San Nicolas de Hidalgo in 1979 and obtained his PhD degree from the University of Canterbury, Christchurch, New Zealand, in 1988.

He was a postdoctoral Fellow at the University of Toronto, Canada, and the University of Durham, UK. He is the Professor of Electrical Power Systems at the University of Glasgow, UK. He is an IEEE PES distinguished lecturer.

Authorized licensed use limited to: Danmarks Tekniske Informationscenter. Downloaded on February 25, 2009 at 10:38 from IEEE Xplore. Restrictions apply.